

COMSOL Implementation of a Porous Media Model for Simulating Pressure Development in Heated Concrete

B. Weber^{*1}, D. Dauti², and S. Dal Pont²

¹Empa, Swiss Federal Laboratories for Material Science and Technology, Dübendorf

²Laboratoire 3SR, University Grenoble Alpes, Grenoble, France

^{*}Benedikt.Weber@empa.ch

Abstract: A model simulating the high temperature behavior of concrete has been implemented in COMSOL using the weak form interface. The model treats concrete as a partially saturated medium and is based on the theory of heat and mass transfer. We show how easily this model can be implemented in COMSOL using a high-level problem definition and automatic differentiation and recursive variable substitution. The model has been implemented in two versions with different sets of dependent variables. The code has been validated by means of an experiment from literature [1]. Moreover, the results of the COMSOL model are compared with our implementation in Cast3M, which also uses a high-level problem definition but lacks the automatic differentiation and substitution of variables. For equal spatial discretization and equal time steps, computational times are comparable for the two softwares.

Keywords: High-performance concrete, Pore pressure, High temperature, Weak form, Dependent variables

1. Introduction

When concrete is subjected to high temperature, capillary water evaporates and chemically bound water is released due to dehydration. This results in an increase of pore pressure, which is believed to be one of the mechanisms leading to spalling. Spalling of concrete is of high concern for the fire safety of concrete structures.

Several models for simulating the high-temperature behavior of concrete have been published in the literature. Most of these models are based on the theory of heat and mass transfer in porous media and have been implemented in specialized finite element codes [2, 3]. As many non-linear phenomena are involved in concrete at high temperature, a fully coupled model is necessary to predict the evolution of temperature and pore pressure. Vapor diffusion, liquid water flow due to pressure gradients, capillary effect,

evaporation/condensation, are the main phenomena observed in a porous medium. Moreover, at high temperatures, dehydration of cement paste occurs which alters the porous structure of concrete and causes the release of free water in the porous network [4]. In addition, the material characteristics of concrete are temperature-dependent. Thus any increase in temperature induces an important change in thermal properties like conductivity, heat capacity, heat of vaporization, and in mass transport properties like permeability, diffusivity, dynamic viscosity.

In a previous publication, we used the physics interfaces to model heat and moisture transfer in heated gypsum [5]. In this paper, however, we used only the weak form interface. The main reason is that we already had a formulation in the weak form that has been implemented in Cast3M. This software is a general finite element code using a script language to implement a model in terms of general building blocks. In contrast to COMSOL all substitutions and derivatives have to be performed manually by the user.

In this work, we consider a model similar to [3] and show how easily it can be implemented in COMSOL using the weak form interface.

2. Mathematical model

Concrete is modelled as a porous multiphase material where the voids of the solid skeleton are filled with liquid and gas. The gas phase is considered to be a mixture of dry air and water vapor.

2.1 Conservation equations

The model is formulated as a coupled system of partial differential equations that describe the mass and energy conservation [6]. The conservation of dry air is:

$$\frac{\partial}{\partial t}(\phi(1-S)\rho_a) + \nabla \cdot (\rho_a \mathbf{v}_a) = 0 \quad (1)$$

Taking into account the mass sources \dot{m}_{dehyd} and \dot{m}_{evap} due to dehydration and evaporation, the conservation of water species (liquid-vapor) reads:

$$\frac{\partial}{\partial t} \phi(S\rho_l + (1-S)\rho_v) + \nabla \cdot (\rho_v \mathbf{v}_v + \rho_l \mathbf{v}_l) = \dot{m}_{\text{dehyd}} \quad (2)$$

Note that the evaporation is a phase change between liquid water and vapor and does not appear explicitly in the conservation of water species.

Conservation of energy is expressed as:

$$\begin{aligned} \rho c_p \frac{\partial T}{\partial t} + \nabla \cdot (-k_{\text{eff}} \nabla T) \\ + (\rho_v c_{pv} \mathbf{v}_v + \rho_a c_{pa} \mathbf{v}_a) \cdot \nabla T \\ = -\dot{m}_{\text{dehyd}} \Delta h_{\text{dehyd}} - \dot{m}_{\text{evap}} \Delta h_{\text{evap}} \end{aligned} \quad (3)$$

where Δh_{dehyd} and Δh_{evap} are the enthalpies related to dehydration and evaporation, respectively. The mass source \dot{m}_{dehyd} due to dehydration is a function depending on temperature, whereas the mass source \dot{m}_{evap} due to evaporation is calculated from the vapor conservation equation:

$$\dot{m}_{\text{evap}} = \frac{\partial}{\partial t} (\phi(1-S)\rho_v) + \nabla \cdot (\rho_v \mathbf{v}_v) \quad (4)$$

For solving the three conservation equations (1)–(3), all variables need to be expressed in terms of three primary variables (dependent variables in COMSOL). Before making a choice for the primary variables, we summarize the additional thermodynamic and constitutive relations we want to use.

2.2 Thermodynamic and transport relations

Assuming dry air and water vapor to behave as ideal gases, the partial densities are described as:

$$\rho_\pi = \frac{P_\pi M_\pi}{RT} \quad \text{for } \pi = a, v \quad (5)$$

where P_π is the pressure, M_π is the molar weight, and R is the universal gas constant. By Dalton's law, the gas pressure is the sum of the partial pressures:

$$P_g = P_a + P_v \quad (6)$$

The gas and the liquid water are assumed to flow under pressure according to Darcy's law. For the gas phase, the velocity is given by:

$$\mathbf{v}_g = -\frac{\kappa_{rg} K}{\mu_g} \nabla p_g \quad (7)$$

and for the capillary water:

$$\mathbf{v}_l = -\frac{\kappa_{rl} K}{\mu_l} \nabla p_l \quad (8)$$

where K is the intrinsic permeability given as a function of temperature and gas pressure; κ_{rl} and κ_{rg} are the phase permeabilities expressed as a function of saturation S [7]; μ_g and μ_l are the temperature-dependent dynamic viscosities for the liquid and gaseous phase.

The model also considers diffusion of dry air and vapor in the gas mixture according to Fick's law:

$$\mathbf{j}_v = -\rho_g D_{\text{eff}} \nabla \left(\frac{P_v}{P_g} \right) = -\mathbf{j}_a \quad (9)$$

where D_{eff} is the effective diffusion coefficient.

2.3 Capillary pressure

As in most porous media, capillary effects play an important role in concrete. Due to surface tension in the curved gas-liquid interface (meniscus), there is a pressure difference between the gas pressure p_g and the liquid pressure p_l . This pressure difference is called capillary pressure:

$$p_c = p_g - p_l \quad (10)$$

The surface tension also has an effect on the vapor saturation. The vapor saturation pressure above a curved liquid-vapor interface is given by means of the Kelvin equation

$$P_v = P_{\text{sat}}(T) \cdot RH = P_{\text{sat}}(T) \cdot \exp \left(\frac{-p_c M_w}{\rho_l RT} \right) \quad (11)$$

The capillary pressure is mainly determined by the pore structure. For a given porous material, we can find the liquid saturation from sorption experiments at different temperatures [8]. The saturation is a function of the relative humidity or, via Equation (11), a function of capillary pressure [2]:

$$S = S(p_c, T) \quad (12)$$

Sorption experiments are typically only available below 100°C and need to be extrapolated for higher temperatures. Here we use the relationship suggested by Gawin et al. [9], which is presented graphically in Figure 1.

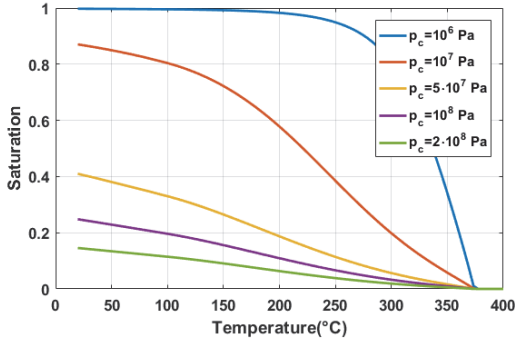


Figure 1. Saturation

2.4 Primary variables

We now come back to the choice of primary variables. While the energy equation is already formulated in terms of temperature, the mass conservation equations need some further development. The gas densities and velocities can be expressed in terms of pressures and pressure gradients by virtue of the relations in Section 2.2.

Taking both the vapor pressure and the saturation as functions of the capillary pressure (Section 2.3), the capillary pressure is a good candidate for one of the two remaining primary variables. The other one is usually taken the gas pressure. The air pressure is then defined from Dalton's law (Eq. (6)) as:

$$P_a = P_g - P_v \quad (13)$$

and the liquid pressure from the definition of the capillary pressure (Eq. (10)) as:

$$P_l = P_g - P_c \quad (14)$$

Assuming incompressibility of the liquid water, the water density is just a function of temperature.

The formulation with the capillary pressure as primary variable appears problematic for temperatures above the critical temperature of water (374°C). The density of liquid water decreases from 1000 kg/m³ at room temperature to 322 kg/m³ at the critical temperature. Above this temperature, liquid and vapor cannot be distinguished and the capillary pressure has no physical meaning anymore. This also invalidates Kelvin's equation for calculating the vapor pressure.

Besides the problem with physics, there is also a numerical issue. When using a polynomial formulation for the water density, extrapolation beyond the critical temperature may result in a zero or even negative water density, which yields

an erroneous vapor pressure from Kelvin's equation (11). To be able to continue the simulation for high temperatures, the liquid density is kept constant above the critical temperature. However, results in this temperature region should be considered with caution. A more elaborate approach considering adsorbed water is given in [2].

An alternative formulation uses the vapor pressure as primary variable. Also this formulation has its limitations, since in the fully saturated state, vapor pressure has no physical meaning. However for the current example, full saturation did not occur and there was no difference in the solutions between the two formulations.

2.5 Boundary Conditions

We consider a rectangular concrete specimen heated on one side by a radiator. As thermal boundary conditions, we have convective and radiative heat exchange simultaneously at the hot and the cold side. The heat flux is:

$$-\mathbf{n} \cdot (-k_{\text{eff}} \nabla T) = h_T (T_{\text{ext}} - T) + \sigma \varepsilon (T_{\text{ext}}^4 - T^4) \quad (15)$$

where h_T is the heat transfer coefficient, σ is the Stefan-Boltzmann constant and ε is the surface emissivity. For the cold side, the temperature T_{ext} corresponds to the room temperature and for the hot side T_{ext} is the temperature of the radiant heater.

Mass transfer boundary conditions are the following. For the gas mixture, the pressure is fixed at atmospheric pressure:

$$P_g = P_{\text{atm}} \quad (16)$$

The vapor transport through the boundary is specified by the vapor flux and is expressed as:

$$-\mathbf{n} \cdot (\rho_v \mathbf{v}_v + \rho_l \mathbf{v}_l) = h_g (\rho_v^{\text{amb}} - \rho_v) \quad (17)$$

where h_g is the mass transfer coefficient. The ambient vapor density is determined from the relative humidity.

3. Use of COMSOL Multiphysics

The coupled system of partial differential equations has been implemented with the COMSOL weak form interface with dependent variables T , P_g , and P_c . The conservation equations (1)–(3) were transformed to the weak form and entered into the program. The other equations were introduced as variables in the defini-

tion node. This is all it takes for the implementation. COMSOL Multiphysics substitutes recursively all variables and their derivatives in the conservation equations until they only depend on material parameters and primary variables. For this to work, Dalton's law and the definition of capillary pressure have to be introduced in the form of Eqs. (13) and (14), respectively.

An alternative implementation using p_v instead of p_c as a primary variable was also implemented. For this implementation, the test functions in the weak form and the initial conditions need to be adapted. Boundary conditions are not affected. In the variables definitions, only the relation between p_v and p_c (Eq. (11)) has to be inverted:

$$p_c = -\frac{\rho_l RT}{M_w} \ln \frac{p_v}{p_{sat}(T)} \quad (18)$$

Thanks to the automatic differentiation and recursive substitution of variables, the rest is done by COMSOL.

The numerical model has also been implemented in the finite element software Cast3M. This software has been developed by the French Alternative Energies and Atomic Energy Commission (CEA) and is freely available for research. Cast3M also uses a high-level implementation but lacks the automatic recursive substitution of variables and evaluation of derivatives. These have to be performed manually which is a cumbersome and time-consuming procedure prone to errors. Therefore, it was not feasible, to implement the alternative formulation with the primary variable p_v .

4. Experimental data

Experimental data are taken from [1]. A concrete plate of 120 mm thickness is heated by a radiant heater placed 3 cm above the upper surface as shown in the experimental setup scheme in Figure 2. The lateral faces of the specimen are insulated with porous ceramic blocks. The specimen contains combined temperature and pressure sensors located at different depths. The concrete was a high performance concrete made with calcareous aggregates and with a compressive strength of 100 MPa.

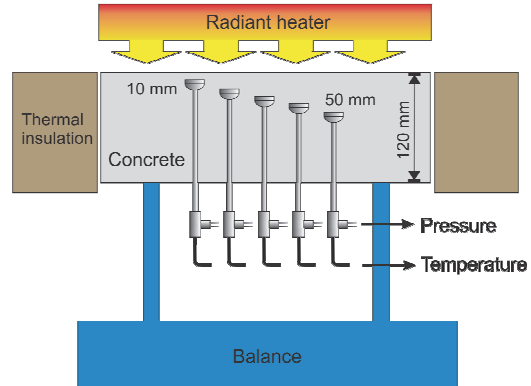


Figure 2. Experimental set up [1]

According to the reference, the heater had a temperature of 600°C. However, detailed information is not available. To match the measured temperatures, it was necessary to use a temperature curve as shown in Figure 3.

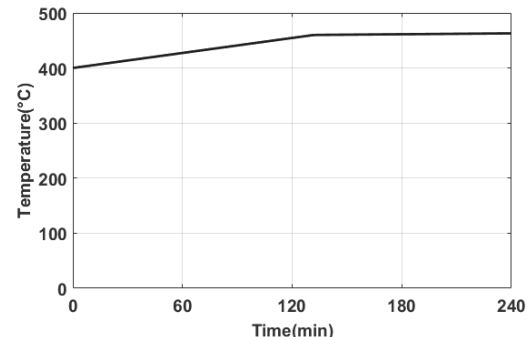


Figure 3. Heating temperature used in numerical simulation

5. Results and discussion

5.1 Comparison with experimental data

Numerical results are compared with experimental results concerning gas pressure and temperature in Figures 4 and 5. The comparison of the temperature fields (Figure 4) shows a good agreement with the experimental observations. When looking at the gas pressure profiles (Figure 5), the position and the value of the peaks are in good agreement with the experiments, except for the pressure values at 30 mm (which is believed to be due to experimental anomalies). However, the width of the curves from the numerical results is wider. The pressure profiles

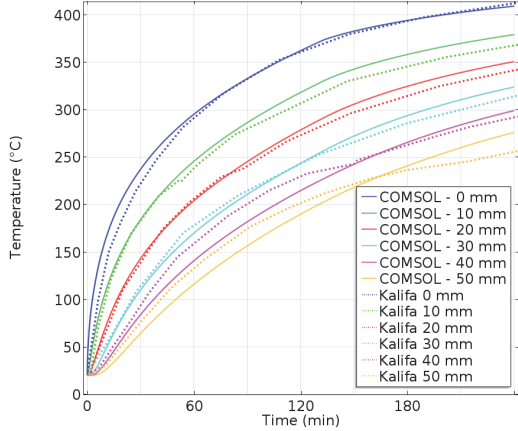


Figure 4. Temperature evolution vs. experiment [1]

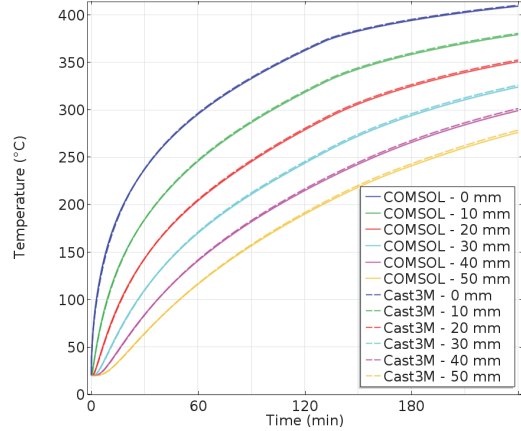


Figure 6. Temperature evolution vs. Cast3M

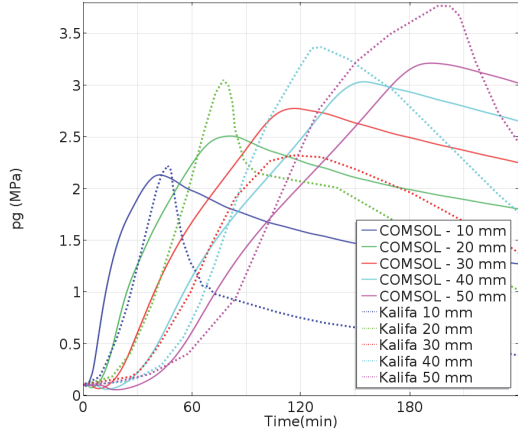


Figure 5. Gas Pressure evolution vs. experiment [1]

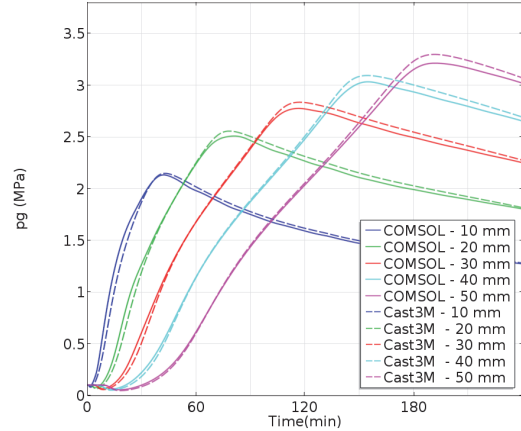


Figure 7. Gas Pressure vs. Cast3M

from the experiments are narrower, due to pressure post peak decrease coming from the formation of cracks, which is not contained in the numerical model.

The model has been developed under version 5.2. The simulations have been performed with a two-dimensional model consisting of 784 elements with quadratic shape functions. To be comparable with Cast3M, calculations have been performed with fixed time steps every 10 sec. Execution time on an Intel Core i7 CPU (quad core) with 2.1 GHz was about 40 minutes. When using the free time stepping feature of COMSOL, the calculation was 6-7 times faster. However, because time steps were sometimes as large as 500 sec, the calculation missed some changes in the constitutive laws, resulting in less smooth curves.

5.2 Comparison with Cast3M

As shown in Figure 6 and Figure 7, COMSOL results compare well with our implementation in Cast3M. In terms of computational efficiency, for a fixed time step the computational time of the two softwares is similar.

5.3 Comparison with alternative model

The calculations were also performed with the alternative formulation using p_v instead of p_c as a primary variable. Results are very similar as shown in the comparison for the gas pressure in Figure 8. Computing time was slightly higher (25%) for the alternative formulation.

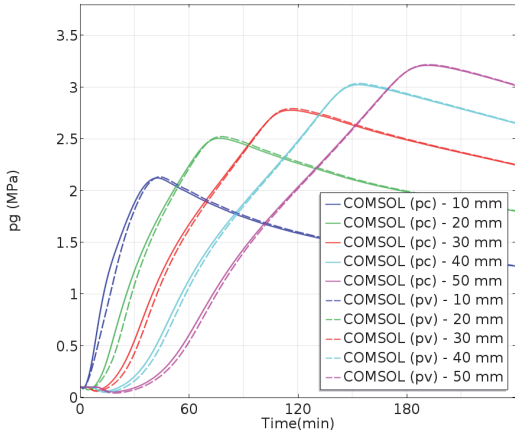


Figure 8. Gas Pressure calculated with two different COMSOL implementations

6. Conclusion

A porous media model for concrete at high temperatures has been implemented with the weak form interface. The conservation equations are entered directly in their weak form. Constitutive equations are entered as expressions in the definitions. The software then takes care of the rest by symbolic evaluation of derivatives and recursive substitution of variables. This mechanism also allows to easily change the dependent variables with only a few modifications.

The model has been applied to an experiment from the literature and is able to reproduce measured temperatures and gas pressures. The alternative model with the vapor pressure as dependent variable yields almost identical results. The COMSOL implementation also compares well with the Cast3M implementation.

7. Nomenclature

c_p	Heat capacity [J/(kg·K)]
D_{eff}	Effective diffusion coefficient [m^2/s]
H	Specific enthalpy [J/kg]
h_T	Heat transfer coefficient [$\text{W}/(\text{m}^2 \cdot \text{K})$]
h_m	Mass transfer coefficient [m/s]
\mathbf{j}	Diffusive mass flux [$\text{kg}/(\text{m}^2 \cdot \text{s})$]
k_{eff}	Effect. thermal conductivity [$\text{W}/(\text{m} \cdot \text{K})$]
\dot{m}	Mass source [$\text{kg}/(\text{m}^2 \cdot \text{s})$]
M	Molar mass [kg/mol]
p	Pressure [Pa]
RH	Relative humidity [-]

S	Saturation [-]
T	Temperature [K]
\mathbf{v}	Velocity [m/s]
Δh	Specific enthalpy of phase change [J/kg]
ε	Surface emissivity [-]
κ_g	Gas permeability [m^2]
μ	Dynamic viscosity [Pa·s]
ϕ	Porosity [-]
ρ	Mass density (partial) [kg/m^3]

8. References

1. Kalifa, P., F.-D. Menneteau, and D. Quenard, Spalling and pore pressure in HPC at high temperatures, *Cement and concrete research*, **30**, 1915-1927 (2000).
2. Gawin, D., F. Pesavento, and B. Schrefler, Modelling of hygro-thermal behaviour and damage of concrete at temperature above the critical point of water, *International Journal for Numerical and Analytical Methods in Geomechanics*, **26**, 537-562 (2002).
3. Dal Pont, S., F. Meftah, and B. Schrefler, Modeling concrete under severe conditions as a multiphase material, *Nuclear Engineering and Design*, **241**, 562-572 (2011).
4. Dal Pont, S. and A. Ehrlacher, Numerical and experimental analysis of chemical dehydration, heat and mass transfers in a concrete hollow cylinder submitted to high temperatures, *International journal of heat and mass transfer*, **47**, 135-147 (2004).
5. Weber, B., *Heat and Mass Transfer in a Gypsum Board Subjected to Fire*, COMSOL conference Stuttgart (2011).
6. Ho, C.K. and S.W. Webb, *Gas transport in porous media*, **20** (2006).
7. Van Genuchten, M.T., A closed-form equation for predicting the hydraulic conductivity of unsaturated soils, *Soil science society of America journal*, **44**, 892-898 (1980).
8. Baroghel-Bouny, V., et al., Characterization and identification of equilibrium and transfer moisture properties for ordinary and high-performance cementitious materials, *Cement and concrete research*, **29**, 1225-1238 (1999).
9. Gawin, D., F. Pesavento, and B.A. Schrefler, What physical phenomena can be neglected when modelling concrete at high temperature? A comparative study. Part 1: Physical phenomena and mathematical model, *International Journal of Solids and Structures*, **48**, 1927-1944 (2011).